Little Tom Thumb among Cells: Seeking the Cues of Life

G. Aletti, P. Causin, G. Naldi and M. Semplice

Abstract For a living being or a cell in a developing body, recognizing its peers and locating food sources or other targets and moving towards them is of paramount importance. In most cases this is achieved by detecting the presence of chemical substances in the environment and moving towards the areas of their higher concentration, a process known as *chemotaxis*. Despite its fundamental role for life, this phenomenon is not yet fully understood in all its details and mathematical models are proving very useful in guiding biological research. We address here two examples of chemotaxis occurring in the developing embryo: early formation of the vascular plexus and axon navigation in the wiring of the nervous system.

1 Introduction

The ability of responding to chemical signals present in the environment is of upmost importance for life, for example to recognize peers or locating food sources. Chemical cues may also serve to mark pathways, which lead to a target (attractive cues) as well as repel from selected regions (repulsive cues). Pathfinding by chemical cues is a key mechanism in the developing embryo, where sets of cells have to organize and reach specific areas to form the different body tissues. Under this aspect, cells behave like "Little Tom Thumbs" of the molecular world. At this scale, cues are represented by single molecules, displaced from their release location by a diffusion process, from higher concentration regions to lower concentration regions. Cells crawl along the concentration gradient, towards (or away from) the direction of increasing chemical signal, moving from the peripheries to the source. This phenomenon is known as *chemotaxis*.

G. Aletti, P. Causin, G. Naldi and M. Semplice
Dipartimento di Matematica "F. Enriques", Università degli Studi di Milano, via Saldini 50, 20133 Milano, Italy, e-mail: aletti,causin,naldi,semplice@mat.unimi.it

Migration of cells was detected from the early days of the development of microscopy, but it was not initially given great importance, since it was, erroneously, not considered as a factor responsible of the patogenicity of microorganisms, which was the main interest at that time. It toke almost a century when in 1881 the German scientist Engelmann observed the movement of bacteria towards the chloroplasts in a strand of *Spirogyra* algae, in response to oxygen generated by the photosynthetically active chloroplasts in the algae. The significance of chemotaxis in biology and clinical pathology was widely accepted in the 1930s, but it was in the 1960s and 1970s that the revolution of modern cell biology and biochemistry provided a series of novel techniques which became available to investigate the migratory response of cells. In particular, the pioneering work of Adler [13] represented a significant turning point in understanding the whole process of intracellular signal transduction of bacteria.

Chemotaxis is at the basis of the self-organization of endothelial cells that, initially born at random positions, will eventually gather to form the capillary network of the embryo. Biologists have detected the presence of a a family of diffusible molecules, named VEGF, that are secreted by endothelial cells and whose gradients is an attractive cue for these same cells (in a so-called autocrine loop, [17]). A mathematical model of the motion of the cells subjected to the VEGF gradient shows that the autocrine loop can be sufficient to explain the formation of a capillary network with a mesh size adequate for the future vital perfusion of oxygen throughout all the tissues.

The migration of neurons necessary to wire up the nervous system is another process which relies on chemotaxis, both of attractive and repulsive type. Neurons detect very small differences in molecule concentration across the tiny section of their distal part, the growth cone, which also internally elaborates the directional signal to perform trajectory decisions. A mathematical model of neuron migration provides hints of the nature of the internal process, that is only partially known to biologists. In particular, it allows to characterize the conditions under which a weak, but coherent, gradient signal can be extracted from the background noise, highlighting the fact that cells work in a substantial balance between deterministic decisions and stochastic behaviour.

2 Chemotaxis in vasculogenesis

The formation of the vascular system in vertebrates starts off in the embryo, when cells initially at random positions differentiate into endothelial cells. Then, they gather into a continuous uniform network of capillaries known as the vascular plexus. This process is known as *vasculogenesis*. An in vitro experiment can be used to reproduce the phases of vasculogenesis, as shown in the microscopy images of Fig. 1. Vasculogenesis requires single endothelial cells to be able to “recognize” their peers and self-organize into a coordinated structure, moving towards other similar cells and connecting up into a network. Recent studies showed that the informa-

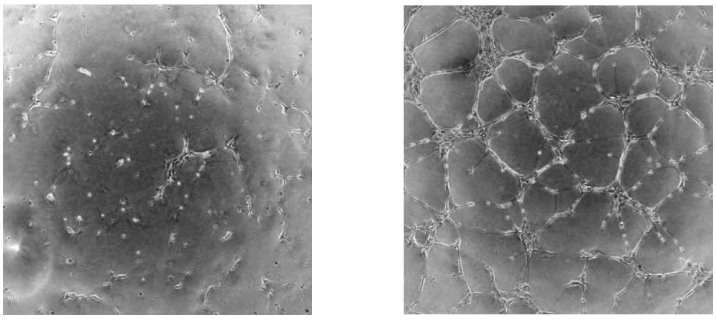

Fig. 1 An *in vitro* vasculogenesis experiment. Endothelial cells are dispersed on a matrigel coated plate (left) and self-organize into a network within few hours (right). Images from [18].

tion carrier during this process is a chemical substance of the VEGF family. In [18], moving endothelial cells were tracked by videomicroscopy and their motion was recognized to exhibit a certain degree of persistence in the direction of motion and a marked tendency to turn towards increasing VEGF gradients. Since not all details of the vasculogenetic process are accessible to direct experimentation, it is important to set up a mathematical model that can be used to run virtual experiments and help biologists to focus on the important issues.

2.1 Mathematical model of vasculogenesis

The mathematical model we deal with concerns the formation of an early vascular network. It is based on the multidimensional Burgers equation, which is a well–known paradigm in the study of pattern formation. It gives a coarse–grained description of the motion of independent agents performing rectilinear motion and interacting only at very short ranges. These equations have been utilized to describe the emergence of structured patterns in many different physical settings (see, *e.g.*, [19, 14]). In the early stages of the dynamics, each particle moves with a constant velocity, assigned by a random statistical distribution. Particle trajectories intersect and shock waves are formed, giving rise to local singularities. Regions of high density grow and form a peculiar network–like structure, which main feature is the existence of comparatively thin layers and filaments of high density that separate large low-density regions. In order to adapt this model to the study of blood vessel formation, one has also to take into account the fact that cells do not behave as independent agents, but rather exchange information in the form of soluble chemical factors. This leads to the models proposed in [9, 18], of which we consider a modified version. We study the evolution of three variables: cell density $n(\mathbf{x},t)$, cell velocity $\mathbf{v}(\mathbf{x},t)$ and VEGF concentration $c(\mathbf{x},t)$ at time t and position $\mathbf{x}$. Let us first concentrate on the chemoattractant dynamics, which is responsible for signalling at each endothelial cell where the others are gathering. VEGF is produced by endothe-

lial cells themselves and spreads around diffusing in the extracellular environment at a speed essentially controlled by its molecular weight. Its behaviour is very much alike that of a metropolitan legend: it has a source (the origin of the piece of news, or the endothelial cell emitting VEGF), diffuses (by the grapevine, or by Brownian motion) and gets degraded exponentially (by the modification of the original news introduced by each person, or by the extracellular environment). Mathematically, this can be described by the evolution equation

$$\frac{\partial c}{\partial t} = D\Delta c + \alpha n - \frac{c}{\tau}, \tag{1a}$$

where D is the diffusion constant, α is the source strength and τ the characteristic time of degradation. Without considering in detail the biochemistry of endothelial cells which leads to motion under a VEGF gradient, here we model this process by the equation

$$\frac{\partial \mathbf{v}}{\partial t} + \mathbf{v}\cdot\nabla\mathbf{v} = \mu\nabla c - \nabla\phi(n) - \beta\mathbf{v}. \tag{1b}$$

The left hand side is the total time derivative of the velocity, while the right hand side describes the forces acting on cells: the chemotactic gradient ∇c, a pressure and a friction term. In order to close the model, we add a further equation enforcing the principle of mass conservation of cells

$$\frac{\partial n}{\partial t} + \nabla\cdot(n\mathbf{v}) = 0. \tag{1c}$$

The three equations (1) constitute a system of partial differential equations. At the heart of the model there is the autocrine loop described by the coupling of the n and c variables in equations (1b) and (1a): VEGF is produced by the very same family of cells that move around following its gradient. The parameters control the relative importance of each term and should depend on c in order to get a realistic model. A more detailed description of the model may be found in [7].

2.2 Fourier analysis

A significant insight in the dynamics predicted by the model can be gained simply using Fourier analysis on system (1), upon setting $\beta = 0$, $\phi(n) = 0$ and assuming constant coefficients. In steady-state conditions, Fourier transforming equation (1a) by substituting the expansion $c(\mathbf{x}) = \sum c_{\mathbf{k}} e^{i\mathbf{k}\cdot\mathbf{x}}$ (and similarly for n), one finds that

$$c_{\mathbf{k}} = \frac{\alpha\tau n_{\mathbf{k}}}{1 + |\mathbf{k}|^2 D\tau}. \tag{2}$$

Thus the forcing term ∇c entering (1b) reads

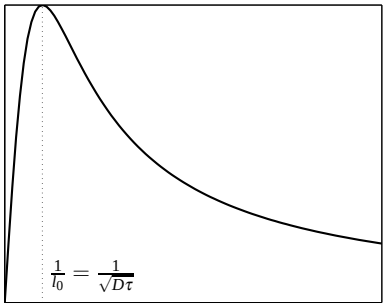

Fig. 2 Amplification factor f for $n_{\mathbf{k}}$ as a function of the wave number $|\mathbf{k}|$.

$$\nabla c_{\mathbf{k}} = |\mathbf{k}| \frac{\alpha \tau n_{\mathbf{k}}}{1 + |\mathbf{k}|^2 D\tau} = \alpha \tau \, f(|\mathbf{k}|) \, n_{\mathbf{k}}, \quad f(x) = \frac{x}{1 + D\tau x^2}. \tag{3}$$

The function $f(|\mathbf{k}|)$ is an amplification factor for $n_{\mathbf{k}}$. Its graph, reproduced in Fig. 2, clearly indicates the net effect of the VEGF autocrine loop: it acts as a filter such that concentration components $n_{\mathbf{k}} e^{i\mathbf{k}\cdot\mathbf{x}}$ with wave vector $\mathbf{k}$ are strengthened if $|\mathbf{k}| \sim 1/\sqrt{D\tau}$ and suppressed otherwise. This implies that the steady state solution should be mainly described by its components with wavelength $l_0 = \sqrt{D\tau}$. Substituting the experimental values of D and τ for VEGF, one gets $l_0 \simeq 200\mu$m, which is -not by chance!- the distance that can be reached by oxygen when perfusing in the tissues from capillaries.

2.3 Simulations and experiments

As observed in [7], realistic models cannot neglect the time derivative in (1a). They should also include all the terms in (1b) and allow a dependence of α, β and μ on the concentration c. Thus, it is not at all obvious that the conclusions of the previous section are still valid in this more complex time-dependent and fully nonlinear setting. This however can be assessed by numerically approximating the solutions of the complete system, after choosing a suitable discretization for the model equations and implementing a simulator in a parallel computing environment (due to the size of the problem).

But what is the initial condition? How should we choose $n(\mathbf{x},0)$, i.e. the initial positions of the endothelial cells? It is unfortunately impossible to follow the embryonal development with non-invasive techniques and thus we cannot get the exact initial positions of the cells. However, biologists know that the endothelial cells are initially approximately randomly scattered in the embryo in the mesoderm germ layer. Thus we set $n(\mathbf{x},0)$ placing cells at randomly chosen positions, state that they

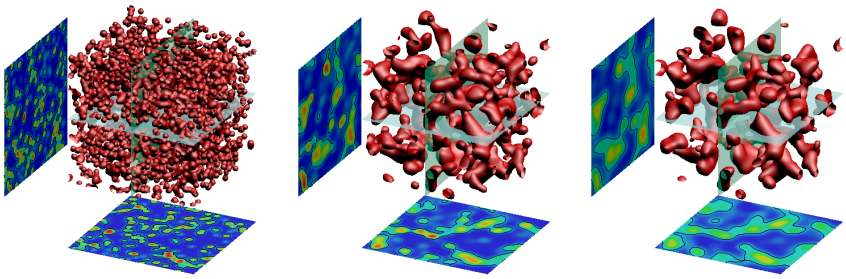

Fig. 3 Initial (left), intermediate (middle) and final (right) cell density configuration from a simulated vasculogenesis experiment. The red surface is an isosurface representing the vessels boundary, while the cross-sections are color-coded representations of the cell concentration.

are initially at rest and that there is no chemoattractant ($\mathbf{v}(\mathbf{x},0) = 0$, $c(\mathbf{x},0) = 0$). This deployes the possibility of comparing the simulations with any given experimental image, since initial values are chosen at random. In order to assess the model behaviour, we run many simulations with different initial data and look for quantities measurable on both the simulations and the experimental images. One of such quantities is the ability of oxygen to perfuse from capillaries into the surrounding tissues. For both the simulations and the experimental data, we mark places where a capillary is present (see [6] for a detailed description). Convoluting the vascular network with a sphere of radius 200μm, tells us whether each region of the embryo can be reached by oxygen perfusing from one of the capillary. Strikingly, results show that real vascular networks are able to oxygenate the whole embryo, while the simulated networks can oxygenate only about 75% of the tissues. This value tells us that the model is a reasonable approximation of the real situation, but also points out its discrepancy. Most likely this is due to the remodelling of the network occurring in later stages, which is not yet taken into account by our model.

3 Chemotaxis in neural development

Wiring up the brain during neural development is a task not so dissimilar from finding (without a cell phone!) a friend who is calling us, lost among the people in a crowd. Neurons extend their distal part, the axon, in search of their targets (the friend, in the analogy), gaining their way through the surrounding tissues. Axon migration can be guided by diffusible chemoattractant substances secreted by intermediate or final targets [22]; the role of chemorepulsion has also been demonstrated by the finding that axons can be repelled by diffusible factors [8]. Different guidance molecules are known to be implicated in this process, including netrins, semaphorins, neurotransmitters (see, *e.g.*, [21, 20]). The growth cone (GC), located at the axon tip, is a highly motile structure that mediates the detection and the transduction of the navigational cues [12, 11]. Chemotropic gradients across the GC

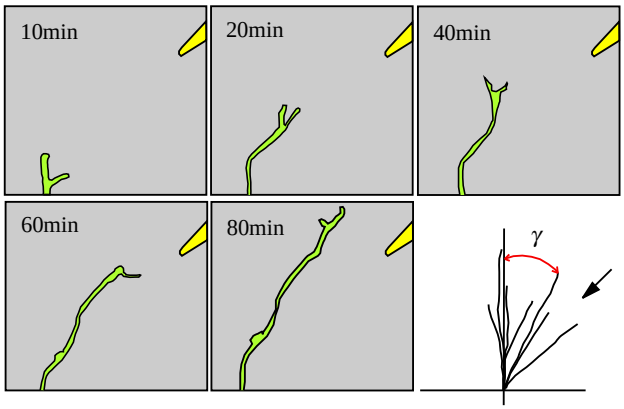

Fig. 4 Chemotactic assay in axon guidance: the pipette, located in the right corner on the top of the figures, establishes a graded field of a chemoattractant and the axon moves towards it (direction of increasing gradient). Experiments record the final turning angle γ for several axon trajectories.

diameter are often quite small. Studies of cultured *Xenopus* spinal neurons showed that the GC can respond to a gradient of diffusible attractants of about $5-10\%$ across its diameter [24, 20]. Despite these shallow gradients, a steeper internal polarization arises in the GC. During the last decade, several studies have focused on deciphering portions of the internal signalling pathway (see, *e.g.*, [20, 12]), which leads to cytoskeleton rearrangement and, ultimately, directional motility [15]. Most of these works are refer to the benchmark *in vitro* chemotactic assay, which analyzes the turning response of GCs exposed to steady graded concentrations of a single attractive/repulsive diffusible cue released by a pipette (see, *e.g.*, [24, 25] and see Fig. 4). We will also consider the same setting.

3.1 Mathematical model of neuron migration

Can we build a model that reproduces the GC behaviour in the chemotactic assay? Which are the most critical parameters? And, above all, is the model able to tell us more about the features of this complex phenomenon, which is still far to be completely unveiled?

Different mathematical and computational models of axon guidance have been developed in the last two decades. Due to the fact that gradient sensing and the internal signal processing are inherently stocastic phenomena, several approaches synthetically describe the GC trajectory using some kind of persistent random walk model (see for example [5, 16]). Further models are investigated in [1, 10, 23], where simple mechanisms are investigated, along with their mathematical properties, that transduce the external signal into an internal signal and then a macroscopic response.

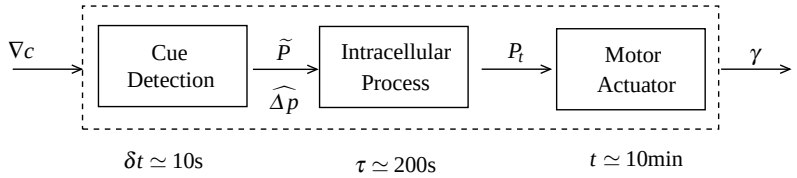

Fig. 5 Functional tasks of the GC transduction cascade: Cue Detection, Intracellular Process and Motor Actuator functions with respective input and output quantities. Characteristics time of each process is indicated under the corresponding box.

To set up our model, we think to the turning process as the sequence of simpler functional tasks. This representation does not reproduces detailed intracellular biochemistry, but it phenomenologically maps input/output signals of each unit (see Fig. 5). Measures of concentration gradients in the environment are produced by the Cue Dectection Subsystem, the Intracellular Process Subsystem receives the input about concentration unbalancings, producing a signal which, through the Motor Actuator Subsystem, causes the deviation of the trajectory. Input and output quantities we refer to in the following are specified in Fig. 5.

3.1.1 Cue detection: listening to our friend's voice

Our friend is calling us: how can we recognize his voice among the others? That is, how do axons "listen to" chemical cues (our friend's voice, in the analogy)? Axons most probably perceive chemotactic gradients using a spatial comparison of ligand concentration across the GC diameter. The work of Berg and Purcell [4] on small sensing devices is an useful theoretical framework to describe signal detection. The sensing devices are represented here by specialized ligand receptors distributed all along the GC surface membrane. If each receptor is capable of binding one molecule of ligand at a time, the probability $\overline{p}$ of the receptor to be bound is

$$\overline{p} = \frac{c}{c + k_D}, \tag{4}$$

where c is the local ligand concentration and k_D its dissociation constant (*i.e*, the concentration for which $\overline{p} = 1/2$). Suppose now that N_1 receptors are concentrated on the side of the GC facing the ligand source and N_2 receptors lie on the other side (see Fig. 6). The history of the i-th site located on side $j = 1$ or $j = 2$ is described by a function $p_j^{(i)}(t)$ that assumes value 1 when the site is occupied and 0 when it is empty. The information about the surrounding concentration is then represented by the processes $p_j^{(i)}(t)$ recorded for a sampling time δt. An approximation of $\overline{p}$ on each side of the GC is given by

$$p_j = \frac{1}{N_i \delta t} \sum_{i=1}^{N_j} \int_{\bar{t}}^{\bar{t}+\delta t} p_j^{(i)}(t)\, dt, \qquad j = 1, 2. \tag{5}$$

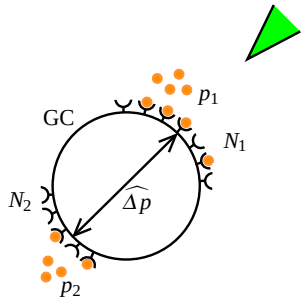

Fig. 6 A graded field of chemoattractant is established across GC sides 1 and 2 by the pipette. The binding states p_1 and p_2 (time average occupation) of the N_1 and N_2 receptors provide an estimate of the concentration difference $\widehat{\Delta p}$.

The difference in occupancy $\widehat{\Delta p} = p_1 - p_2$ provides an estimate of the difference of concentration across sides 1 and 2. We will come back to this this quantity at the end of Sect. 3.1.2.

3.1.2 Climbing up the transduction chain

Hearing the voice of our friend is just the beginning of the process. A large amount of work must then be performed to reach him. This work is for the most part hidden from the experimental observation (we just observe the motion). However, some insight can be gained from the mathematical model. We can characterize the degree of organization of the signal through the hidden steps of the chain using descriptive statistical indexes. Starting from the experimental measures of turning angles in the chemotactic assay and using the mathematical model, we can proceed back and compute indexes of the earlier compartments. As a statistical index, we use the coefficient of variation, defined as the ratio between the standard deviation $\mathrm{std}(\cdot)$ and the expected value $\mathbb{E}(\cdot)$ of a stochastic distribution. Its value allows to assess the weight of the fluctuating over the deterministic part of the signal. Referring to the data of [24] (comparable values are obtained from similar experiments by other authors) for axon turning angles γ (see Fig. 4 for the definition), we compute

$$\mathrm{CV}_\gamma = \frac{\mathrm{std}(\gamma)}{\mathbb{E}(\gamma)} \simeq 1.16,$$

where a time of $2h$ is considered for the observations. The model allows to relate CV_γ to the coefficient of variation CV_{P_t} of the output P_t of the intracellular process. The quantity P_t represents an equivalent force vector that alters the mechanical balance of the GC trajectory. It is a stochastic variable composed of a deterministic part $\widehat{P}$, which is an "exact" (deterministic) response to the gradient, and a random noise term, due to fluctuations and errors in the transduction process. We get (see [2] for a detailed mathematical derivation)

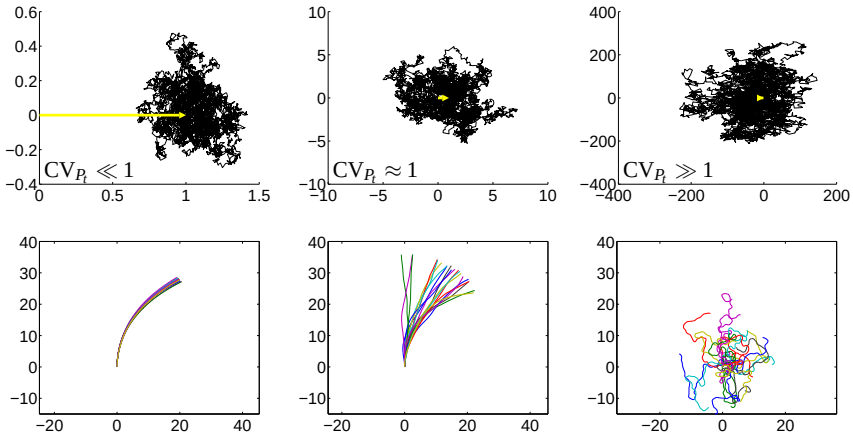

Fig. 7 Top row: time evolution of $P_t^* = P_t/|\widehat{P}|$ of a typical sample at $t = 40\tau$. The arrow in each panel is the ideal force $\widehat{P}^* = \widehat{P}/|\widehat{P}|$ (scales in each panel are different, dimensionless units). Bottom row: corresponding trajectories of 50 out of 10000 computer simulations (scales in μm).

$$\mathrm{CV}_{P_t} \approx \sqrt{\frac{t}{2\tau}}\mathrm{CV}_\gamma \simeq 5, \tag{6}$$

τ being the time parameter of the intracellular process. Since Eq. (6) leads to a value of CV_{P_t} of the order of the unity, this suggests that stochastic and deterministic effects act with comparable magnitude in the internal function. This mechanism represents a "robust" process with respect to fluctuations: the underlying directional message is functionally preserved, despite the significant presence of noise.

It is interesting to use the model to study more in detail the effect of the value of CV_{P_t} on the GC trajectory. We consider the regimes $\mathrm{CV}_{P_t} \ll 1$, $\mathrm{CV}_{P_t} \approx 1$ and $\mathrm{CV}_{P_t} \gg 1$. In Fig. 7 (top row), we show the simulated processes P_t due to a cue directed along the positive x-axis at time $t = 40\tau$ (the system has fairly achieved its steady state). The dimensionless quantity $P_t^* = P_t/|\widehat{P}|$ is plotted for convenience. When $\mathrm{CV}_{P_t} \ll 1$, the process exponentially drifts to the target value (1,0) remaining confined in a narrow neighborhood of this latter so that a macroscopic motion with a deterministic nature is expected. On the contrary, when $\mathrm{CV}_{P_t} \gg 1$, we expect a totally random walk, since noise is dominating. When $\mathrm{CV}_{P_t} \approx 1$, the drift and the volatility effects are in competition. In Fig. 7 (bottom row), we plot the corresponding simulated macroscopic GC trajectories (50 trajectories out of 10000 simulations), which display a very different level of coherency depending on the magnitude of CV_{P_t}. The central panel reproduces more faithfully the typical results of laboratory experiments (see, e.g., [24]), supporting the idea that $\mathrm{CV}_{P_t} \approx 1$ is the characteristic operational regime of the internal process. We can proceed further to investigate the properties of first part of the chain, the cue detection function. With this aim, we introduce the quantity ℓ, which is connected to the ratio between the variability of the output of the intracellular process subsystem and of the cue de-

tection subsystem. Let σ_1^2 and σ_2^2 be the variances of a typical sensing process on side 1 or 2 of the GC. Setting $N_1 = N_2 = N$ and using Eq. (6), we get (see [3] for details)

$$\ell = \sqrt{\frac{Nt}{\delta t}} \frac{\mathbb{E}(\widehat{\Delta p})}{\sqrt{\sigma_1^2 + \sigma_2^2}} \mathrm{CV}_\gamma, \tag{7}$$

where $\mathbb{E}(\cdot)$ is the expected value of a variable. Eq. (7) connects the first and the last part of the chain and can be used to predict (without entering a laboratory!) the statistical indexes of different experimental settings. For example, we can study what happens for a ligand concentration x, with respect to the reference concentration k_D, obtaining (see [3] for details)

$$\frac{\mathrm{CV}_{\gamma|_x}}{\mathrm{CV}_{\gamma|_{k_D}}} = \frac{\frac{\mathrm{Var}_{\widetilde{P}|_x}}{\mathrm{Var}_{\widetilde{P}|_{k_D}}} + (\ell^2_{|_{k_D}} - 1)}{\ell^2_{|_{k_D}}} \frac{\mathbb{E}(\widetilde{P}_{|_x})}{\mathbb{E}(\widetilde{P}_{|_{k_D}})}, \tag{8}$$

where $\mathrm{Var}_{\widetilde{P}_x}$ is the variance of the signal in output from the cue dectection box at concentration x. This allows to propose experimental settings that the biologist can be interested to test and that otherwise could be disregarded.

4 Conclusions

Biological phenomena are often too complex to be directly observed. The environment where they take place is rich of concurring processes. Mathematical models offer the possibility of performing *in silico* experimentations under controlled conditions of graded complexity: their goal is not just to reproduce the laboratory results, the "shape", but, more usefully, to provide explanations of the "function", offering to the biologist real new insights. When deciding what is the most appropriate mathematical model, one must consider the fact that biological phenomena are inherently stochastic, since, just to cite one reason, at the scale at which they take place thermal fluctuations are relevant. It is however necessary to take into account what is the information we are looking for. On the one hand, a purely deterministic PDE approach picks the main features of the process and computes average quantities, providing a macroscopic information (for example, the diffusion length in the vasculogenesis simulation), which may help in assessing biological hypotheses. On the other hand, a purely stochastic model studies fluctuations around average behaviours. As such, it might be more indicated if one wants, for example, to understand the reproducibility of a phenomenon and practically evaluate the number of experiments that must be carried out to obtain significativity (see Eq. (8)). Models that combine both deterministic and stochastic elements, here not extensively addressed, are more delicate and represent an useful tool to study nonlinear phenomena, where fluctuations have a strong impact. One problem of this kind, which will be the object of forthcoming work, is amplification of weak chemotactic signals in axon guidance.

References

1. Aeschlimann, M., Tettoni, L.: Biophysical model of axonal pathfinding. Neurocomputing **38–40**, 87–92 (2001)
2. Aletti, G., Causin, P.: Mathematical characterization of the transduction chain in growth cone pathfinding. IET Sys Biol **2(3)**, 150–161 (2008)
3. Aletti, G., Causin, P., Naldi, G.: A model for axon guidance: sensing, transduction and movement. In: L.M. Ricciardi et al. (ed.) *AIP Proceedings*, vol. 1028, pp. 129–146 (2008)
4. Berg, H., Purcell, E.: Physics of chemoreception. Biophys.J. **20**, 193–219 (1977)
5. Buettner, H.M., Pittman, R.N., Ivins, J.: A model of neurite extension across regions of nonpermissive substrate: simulations based on experimental measurements of growth cone motility and filopodial dynamics. Dev. Biol. **163**, 407–422 (1994)
6. Cavalli, F., Gamba, A., Naldi, G., Oriboni, S., Semplice, M., Valdembri, D., Serini, G.: Modelling of 3D early blood vessel formation: simulations and morphological analysis. In: L.M. Ricciardi et al. (ed.) *AIP Proceedings*, vol. 1028, pp. 311–327 (2008)
7. Cavalli, F., Gamba, A., Naldi, G., Semplice, M., Valdembri, D., Serini, G.: 3D simulations of early blood vessel formation. J. Comput. Phys. **225**, 2283–2300 (2007)
8. Fitzgerald, M., Kwiat, G., Middleton, J., Pini, A.: Ventral spinal cord inhibition of neurite outgrowth from embryonic rat dorsal root ganglia. Development **117**, 1377–1384 (11993)
9. Gamba, A., Ambrosi, D., Coniglio, A., de Candia, A., Di Talia, S., Giraudo, E., Serini, G., Preziosi, L., Bussolino, F.: Percolation, morphogenesis, and Burgers dynamics in blood vessels formation. Phys. Rev. Lett. **90**, 118,101 (2003)
10. Goodhill, G.J., Gu, M., Urbach, J.S.: Predicting axonal response to molecular gradients with a computational model of filopodial dynamics. Neural Comp. **16**, 2221–2243 (2004)
11. Gordon-Weeks, P.: Neuronal growth cones. Cambridge University Press (2000)
12. Guan, K., Rao, Y.: Signalling mechanisms mediating neuronal responses to guidance cues. Nature Rev. Neurosci. **4**, 941–956 (2003)
13. Julius Adler, J., Tso, W.: Decision-making in bacteria: Chemotactic response of Escherichia Coli to conflicting stimuli. Science **184**, 1292–1294 (1974)
14. Kardar, M., Parisi, G., Zhang, Y.: Dynamical scaling of growing interfaces. Phys. Rev. Lett. **56**, 889–892 (1986)
15. Luo, L.: Actin cytoskeleton regulation in neuronal morphogenesis and structural plasticity. Annu. Rev. Cell Dev. **18**, 601–635 (2002)
16. Maskery, S.M., Shinbrot, T.: Deterministic and stochastic elements of axonal guidance. Annu. Rev. Biomed. Eng. **7**, 187–221 (2005)
17. Seghezzi, G., Patel, S., Ren, C., Gualandris, A., Pintucci, G., Robbins, E., Shapiro, R., Galloway, A., Rifkin, D., Mignatti, P.: Fibroblast growth factor-2 (FGF-2) induces vascular endothelial growth factor (VEGF) expression in the endothelial cells of forming capillaries: an autocrine mechanism contributing to angiogenesis. J. Cell Biol. **141**, 1659–1673 (1998)
18. Serini, G., Ambrosi, D., Giraudo, E., Gamba, A., Preziosi, L., Bussolino, F.: Modeling the early stages of vascular network assembly. EMBO J. **22**, 1771–1779 (2003)
19. Shandarin, S., Zeldovich, Y.: The large-scale structure of the universe: turbulence, intermittency, structures in a self-gravitating medium. Rev. Mod. Phys. **61**, 185–220 (1989)
20. Song, H., Poo, M.M.: The cell biology of neuronal navigation. Nat. Cell Biol. **3**, E81–E88 (2001)
21. Tessier-Lavigne, M., Goodman, C.: The molecular biology of axon guidance. Science **274**, 1123–1133 (1996)
22. Tessier-Lavigne, M., Placzek, M., Lumsden, A.G., Dodd, J., Jessell, T.M.: Chemotropic guidance of developing axons in the mammalian nervous system. Nature **336**, 775–778 (1988)
23. Xu, J., Rosoff, W., Urbach, J., Goodhill, G.: Adaptation is not required to explain the long–term response of axons to molecular gradients. Development **132**, 4545–4562 (2005)
24. Zheng, J.Q., Felder, M., Connor, J.A., Poo, M.: Turning of nerve growth cone induced by neurotransmitters. Nature **368**, 140–144 (1994)
25. Zheng, J.Q., Wan, J., Poo, M.: Essential of role of filopodia in chemotropic turning of nerve growth cone induced by a glutamate gradient. J. Neurosci. **16(3)**, 1140–1149 (1996)